Supplemental Document

Optics EXPRESS

Color computational ghost imaging based on a plug-and-play generalized alternating projection: supplement

SHOUPEI LIU,[1,2] QI LI,[1,2] HUAZHENG WU,[1] AND XIANGFENG MENG[1,*]

[1] *School of Information Science and Engineering, Shandong Provincial Key Laboratory of Laser Technology and Application, and MOE Key Laboratory of Laser & Infrared Systems, Shandong University, Qingdao 266237, China*
[2] *Equal contributors.*
[*] *xfmeng@sdu.edu.cn*

Supplement DOI: https://doi.org/10.6084/m9.figshare.19709392

Parent Article DOI: https://doi.org/10.1364/OE.459488

Color computational ghost imaging based on plug-and-play generalized alternating projection：supplement

SHOUPEI LIU,[1,2] QI LI,[1,2] HUAZHENG WU,[1] AND XIANGFENG MENG[1*]

[1]*School of Information Science and Engineering, Shandong Provincial Key Laboratory of Laser Technology and Application, and MOE Key Laboratory of Laser & Infrared Systems, Shandong University, Qingdao 266237, China*
[2] *These authors contributed equally*
**xfmeng@sdu.edu.cn*

This document provides supplementary information to "Color computational ghost imaging based on plug-and-play generalized alternating projection". We provide more information including: the quantitative evaluation of different color computational ghost imaging (CGI) reconstruction algorithms, the proposed method using different denoising algorithms, the proposed method using different demosaicking algorithms in simulation, and the quantitative evaluation of different reconstruction algorithms in experiments.

1. Quantitative evaluation of different color CGI reconstruction algorithms in simulations

To quantitatively compare the reconstruction results of different algorithms, we introduce two metric functions, the peak signal to noise ratio (PSNR) and the structural similarity index (SSIM). PSNR is the most popular objective method for evaluating image quality and SSIM is used to measure the similarity of two images. Their formulas are as follows:

$$PSNR = 10 \times \log_{10}\left(\frac{(2^n - 1)^2}{MSE}\right), \tag{1}$$

$$MSE = \frac{1}{3 \times M}\sum_{j}\sum_{x,y}\left(\widehat{O_j}(x,y) - O_j(x,y)\right), \tag{2}$$

$$SSIM = \frac{(2\eta_{\hat{O}}\eta_O + c_1)(2\sigma_{\hat{O}O} + c_2)}{(\eta_{\hat{O}}^2 + \eta_O^2 + c_1)(\sigma_{\hat{O}}^2 + \sigma_O^2 + c_2)}, \tag{3}$$

where n is the bit depth, η and σ^2 represent the mean and variance of the image, respectively. $\sigma_{\hat{O}O}$ stands for the covariance between the reconstructed color image and the groundtruth and c_1, c_2 are the regularization parameters. The quantitative evaluation curves of the color reconstructed images are shown in Fig. S1. Overall, the PSNR and SSIM of the reconstructed images obtained by different algorithms increase with the increase of the sampling ratio (SR) in both target color images. This indicates that the loss of image quality caused by the reduction of SR is inevitable. Compared with the other three algorithms, the proposed method has better reconstruction quality under different SRs, so its PSNR and SSIM curves are always at a higher position. Consistent with the restored results, it is difficult for the correlation algorithm to reconstruct a clear image, and the corresponding metric functions values are extremely low, even in the case of full sampling. Although the conventional plug-and-play generalized alternating projection (PnP-GAP) and compressed sensing ghost imaging (CSGI) algorithms perform well when SR is 1, both of their curves are steeper and fall faster. This shows that the decrease in SR makes restored images have a more serious loss of image quality, especially the color information. In the process of reconstructing mosaic images through multiple iterative optimizations, the Bayer color mask used to encode color information is seriously damaged and difficult to reconstruct completely. Therefore, it is difficult to restore the original color information. The PSNR and SSIM curves of the reconstructed images by the algorithm of a pre-trained deep demosaicking network (DDN) [1] embedding into PnP-GAP iteration are smoother overall. For simple images, such as the "bird" used in the simulation, when the SR is as low as 0.0625, the PSNR is above 24 and the SSIM is above 0.8. In this case, the reconstructed images quality is even higher than that of the fully sampling CSGI, which is equivalent to the SR of 0.6 or even higher for the traditional PnP-GAP algorithm. For target color images with more detailed information, the proposed algorithm can also achieve PSNR values above 18 and SSIM above 0.6. It indicates that the algorithm can also recover high-frequency detail information well, and more importantly, the color information is always close to the original images.

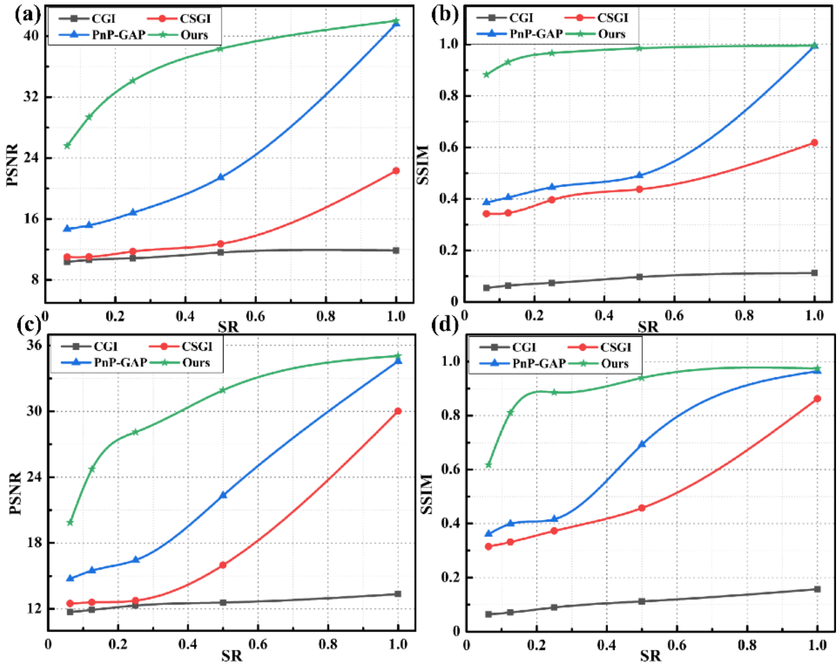

Fig. S1. Quantitative evaluation of different reconstruction methods in simulation. (a), (b) The PSNR and SSIM curves of the “bird”. (c), (d) The PSNR and SSIM curves of the “STOP”.

2. Quantitative evaluation of the proposed method using different denoising algorithms in simulations

Due to the flexibility of the PnP-GAP algorithm, different denoising algorithms can be replaced during the iterative loop to produce different results. Therefore, it is crucial to test the performance of the proposed method under different denoising algorithms. Four denoising algorithms, bilateral filtering [2], wavelet filtering [3], TV [4], and FFD-Net [5], are used as denoising priors in the PnP-GAP to reconstruct the color image “bird”. Embedded in the PnP-GAP algorithm is still the deep demosaicking network DDN. The PSNR and SSIM of the reconstructed images at different SRs are shown in Fig. S2. Different denoising algorithms do not change the trend that the larger the SR, the better the quality of the reconstructed images. The four denoising algorithms can obtain high-quality reconstruction results at full sampling, with PSNR above 20 and SSIM above 0.8. Among them, the reconstruction quality of the bilateral filtering method is the worst, but its quality decreases slowly, and it is obviously better than the wavelet denoising algorithm when the SR is lower than 0.3. PnP-GAP based on TV denoising priors outperforms both significantly. At the SR of 0.0625, PSNR is 8 higher than bilateral filtering and SSIM is 0.2 higher. However, using the pre-trained deep denoising network significantly outperforms the other three algorithms at every SR. There is also less reduction in image quality due to lower SR. Traditional model-based denoising algorithms apply hand-crafted image priors, which lack applicability to image structures with complex features, and the applicable noise types are relatively single. In contrast, pre-trained FFD-Net utilizes a large set of data for training and more effectively extracts prior information from images. It can handle different noise levels and spatially variant noise more flexibly.

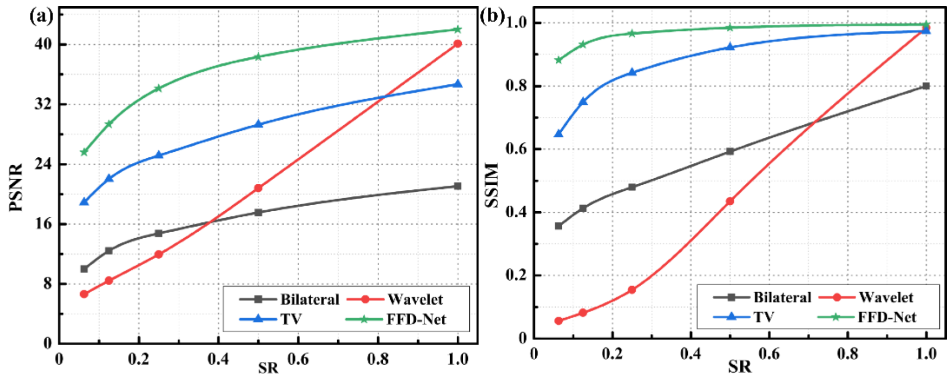

Fig. S2. Quantitative evaluation of the proposed method using different denoising algorithms in simulation. (a) The PSNR curve. (b) The SSIM curve.

3. Quantitative evaluation of the proposed method using different demosaicking algorithms in simulations

Similarly, the color image "bird" is reconstructed by embedding different demosaicking algorithms into the PnP-GAP to compare their reconstruction performance. Four different demosaicking algorithms, bilinear interpolation [6], Malvar (2004) [7], Menon (2007) [8], and DDN are used to recover the color information of the images. The denoising prior used in PnP-GAP is all FFD-Net denoising algorithm. The PSNR and SSIM of the reconstructed images at different SRs are shown in Fig. S3. The different demosaicking algorithms do not seriously degrade the reconstruction quality of the images. When the SR is as low as 0.0625, the PSNR can reach above 14, and the SSIM can reach above 0.6. Among them, the classical bilinear interpolation demosaicking algorithm has the worst reconstructed image quality. The reconstruction results using the DNN-based demosaicking algorithm are significantly better than the other three algorithms, which significantly improves the image quality. Most of the traditional demosaicking algorithms are based on hand-crafted priors, and there will be some inevitable visual artifacts in the reconstruction, thus reducing the image quality. However, the powerful DNN model allows us to learn the adaptively demosaicking priors directly from a large number of training images rather than learning or predefining some hand-crafted priors, which enables better performance on demosaicking tasks.

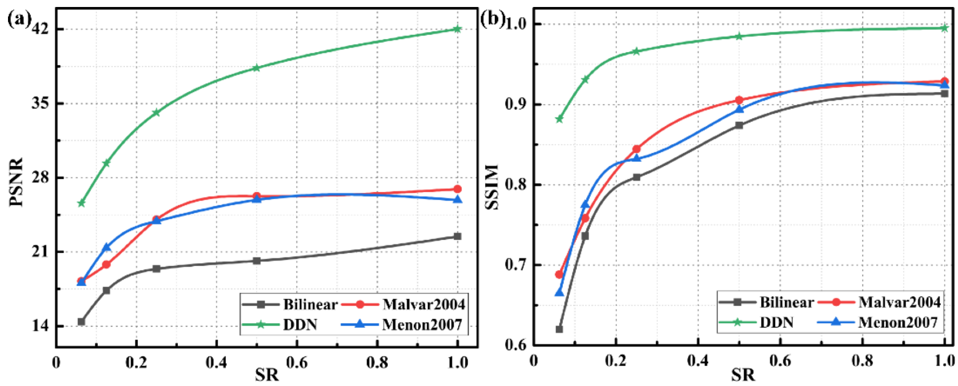

Fig. S3. Quantitative evaluation of the proposed method using different demosaicking algorithms in simulation. (a) The PSNR curve. (b) The SSIM curve.

4. Quantitative evaluation of different color CGI reconstruction algorithms in optical experiments

To quantitatively evaluate the reconstruction performance, the PSNR and SSIM of the reconstructed images in different algorithms are calculated separately for "SDU". The curves are shown in Fig. S4. The PSNR and SSIM of the reconstructed images obtained by the classical correlation-based CGI algorithm are in a relatively low range. Due to the simple image structure and color distribution of the letters “SDU”, the evaluation curves obtained by CSGI and conventional PnP-GAP algorithms are not much different. The evaluation curves obtained by the proposed method are in the highest position. The PSNR is higher than 20, and the SSIM is all above 0.6. The curves prove that the proposed method has the best performance in color CGI experimental reconstructions. In addition, the lack of color correction will also degrade the image quality to some extent.

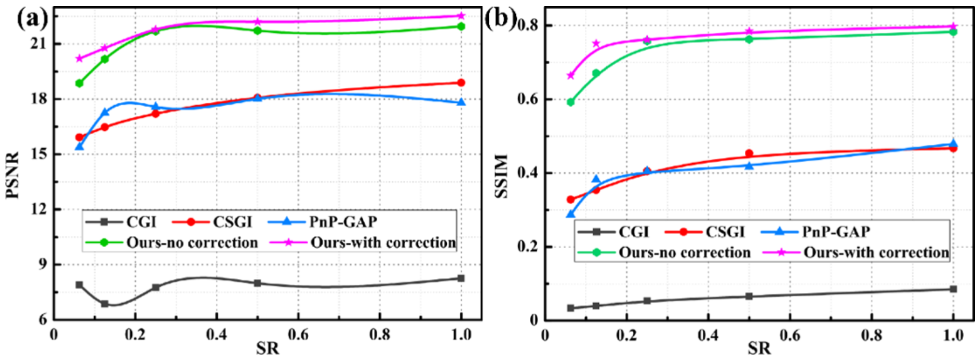

Fig. S4. Quantitative evaluation of different reconstruction methods in experiments. (a), (b) The PSNR and SSIM curves of the “SDU”.

References:

1. R. J. Tan, K. Zhang, W. M. Zuo, and L. Zhang, “Color image demosaicking via deep residual learning,” in Proc. IEEE Int. Conf. Multimedia Expo, 793-798 (2017).
2. C. Tomasi and R. Manduchi, “Bilateral filtering for gray and color images,” in Proc. IEEE Int. Conf. Comput. Vis., 839–846 (1998).
3. S. Mallat and W. L. Hwang, “Singularity detection and processing with wavelets,” IEEE T. Inform. Theory **38**(2), 617–623 (1992).
4. X. Yuan, “Generalized alternating projection based total variation minimization for compressive sensing,” in Proc. IEEE Int. Conf. Image Process., 2539–2543 (2016).
5. K. Zhang, W. Zuo, and L. Zhang, “FFDNet: Toward a fast and flexible solution for cnn-based image denoising,” IEEE T. Image Process. **27**(9), 4608–4622 (2018).
6. J. E. Adams, “Interactions between color plane interpolation and other image processing functions in electronic photography,” in Proc. IS&T/SPIE Symp. Electron. Imag., Sci. Technol. **2416**, 144–151 (1995).
7. H. S. Malvar, L. W. He, and R. Cutler, “High-quality linear interpolation for demosaicing of Bayer-patterned color images,” in Proc. IEEE Int. Conf. Acoust. Speech Signal Process., 485–488 (2004).
8. D. Menon, S. Andriani, and G. Calvagno, “Demosaicing with directional filtering and a posteriori decision,” IEEE T. Image Process. **16**, 132–141 (2007).